J Therm Anal Calorim (2010) 100:751–756
DOI 10.1007/s10973-010-0677-0

Effect of zinc(II) doping on thermal and optical properties of potassium hydrogen phthalate (KHP) crystals

S. Parthiban · S. Murali · G. Madhurambal · S. P. Meenakshisundaram · S. C. Mojumdar

CTAS2009 Special Chapter
Received: 27 December 2009 / Accepted: 7 January 2010 / Published online: 18 February 2010

Abstract The influence of doping the transition metal Zn(II) on potassium hydrogen phthalate (KHP) crystals has been studied. A close observation of FT-IR and XRD profiles of doped and undoped samples reveals some minor structural variations. It appears that the crystal undergoes considerable lattice stress as a result of doping the bivalent zinc. Furthermore, the possibility of cation vacancies aroused owing to the substitution of K^{1+} by Zn^{2+} could result in a defective crystal system. Energy dispersive spectra reveal the incorporation of Zn(II) in the crystalline matrix of KHP crystals. Differential scanning calorimetry (DSC) and TG-DTA studies reveal the purity of the sample and no decomposition is observed below the melting point. Small quantity additions of Zn(II) enhance the fluorescence intensity of KHP crystals. The doping results in morphological changes and significantly improves the second harmonic generation (SHG) efficiency of the host crystal.

Keywords Nonlinear optical materials · Zinc doping · DSC · TG · DTA · KHP · SHG · Zn(II)

S. Parthiban · S. Murali · S. P. Meenakshisundaram
Department of Chemistry, Annamalai University, Annamalainagar 608 002, India

G. Madhurambal
Department of Chemistry, ADM College for Women, Nagapattinam, India

S. C. Mojumdar (✉)
Department of Engineering, University of New Brunswick, Saint John, NB E2L 4L5, Canada
e-mail: scmojumdar@yahoo.com; subhash.mojumdar@yahoo.com

Introduction

Potassium hydrogen phthalate (KHP) crystal is well known for its application in the production of crystal analyzer for long wave X-ray spectrometer [1, 2]. KHP possesses piezoelectric, pyroelectric, elastic, and nonlinear optical (NLO) properties [3–5]. It crystallizes in orthorhombic structure with space group $Pca2_1$ [6]. It has platelet morphology with perfect cleavages along (010) plane. Using the periodic bond chain analysis, the morphology of KHP has been determined [7]. Recently, KHP crystals are used as substrates for the growth of highly oriented film of conjugated polymers with nonlinear optical susceptibility [8, 9]. KHP is chosen as model compound because of its well-developed surface pattern on the (010) face consisting of high and very low growth steps which can be relatively easily observed by means of optical microscopy [10, 11].

The Zn-doped III–V semiconductor layers have been proposed in the last decades as materials for a wide range of opto-electronic device [12]. Incorporation of small amounts of zinc in polycrystalline $CuInS_2$ thin films for solar cells leads to an increased open circuit voltage [13]. The rate of degradation of Zn-doped WO_3 thin films were enhanced in aqueous NaCl solutions [14]. The introduction of a small quantity of Zn^{2+} proved to play an important role in directing the anisotropic growth of SnO_2 nanocrystals. Further branched Zn-doped SnO_2 nanorod clusters with tunable size and aspect ratios were prepared by a facile solvothermal process [15]. The weak temperature dependence of the pinning potential for Zn-doped YBCO crystals at low temperatures shows drastic and systematic changes in U_0 at higher temperatures [16].

Recently, we have investigated the influence of alkaline earth and transition metals doping on the properties and

crystalline perfection of KHP crystals [17]. It is interesting to observe that the alkaline earth metal Mg occupies predominantly substitutional positions while the transition metal Hg mainly occupies the interstitial sites. Accommodating capability of ADP crystals with dopants like KCl and oxalic acid reveals some interesting features [18]. Influence of Mn(II) doping on the NLO properties of ZTS reveals a good correlation of SHG efficiency and the crystalline perfection [19]. Thermal, X-ray, microscopic and spectral analyses are very useful techniques for materials characterization. Therefore, many authors have used these techniques for a variety of materials characterization [20–45]. As a continuation of our previous studies to ascertain the influence of doping on the KHP properties, this work has been undertaken. In the present investigation, we have used Zn(II), a transition metal for doping and the effects on properties of KHP crystals are systematically studied.

Experimental

Synthesis and crystal growth

Potassium hydrogen phthalate crystals were grown from high purity salt. Solubility of KHP was maintained in the temperature range 30–35 °C and the growth solution was prepared according to the solubility data. A small quantity of dopant, Zn(II) (0.0005–0.012 mol dm^{-3}) in the form of $ZnSO_4$ was used for doping. The solution was stirred at 30 °C and slow evaporation method was used for the growth of the crystals from aqueous solution. Photographs of the crystals grown from pure and zinc-doped KHP at different concentrations are shown in Fig. 1.

The FT-IR spectra were recorded for all the samples including pure KHP using an AVATAR 330 FT-IR instrument using the KBr pellet technique in the range 500–4000 cm^{-1}. The powder diffraction analysis was performed using Philips Xpert Pro Triple-axis X-ray diffractometer. Single-crystal X-ray diffraction is an analytical technique which uses the diffraction pattern produced by bombarding a single crystal with X-rays to solve the crystal structure. This analysis was performed using an ENRAF–NONIUS CAD 4 instrument. The XRD data is analyzed by Rietveld method with RIETAN-2000. The surface morphology and amount of incorporated dopant content were observed using a JEOL JSM 5610 LV scanning electron microscope. In the SEM, the image is formed and presented by a very fine electron beam, which is focused on the surface of the specimen. At any given moment, the specimen is bombarded with electrons over a very small area. Fluorescence (PL) spectra were measured on an ELICO fluorescence instrument. TG-DTA–DSC curves were recorded on a SDT Q600 (TA instrument) thermal analyzer. The TG-DTA curves were simultaneously obtained in nitrogen at a heating rate of 10 °C min^{-1}. The DSC analysis of crystals grown from pure and Zn(II)-doped KHP solutions was carried out between 50 and 400 °C in the nitrogen atmosphere.

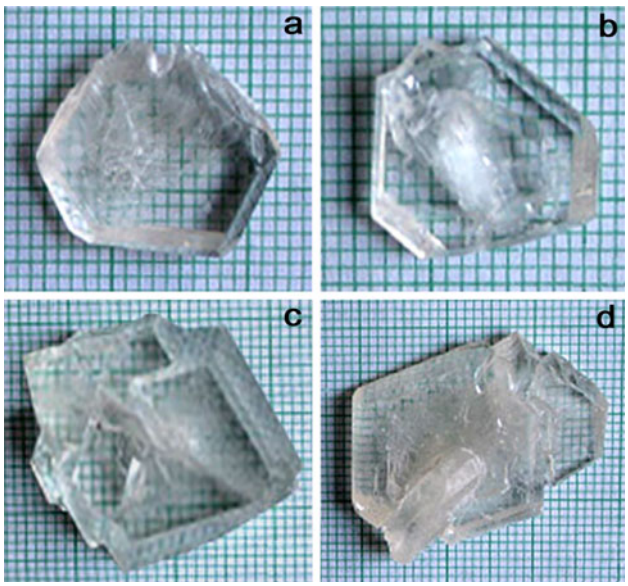

Fig. 1 Photographs of KHP as-grown crystals. **a** Pure, **b** 0.0005 mol dm^{-3} Zn(II) doped, **c** 0.003 mol dm^{-3} Zn(II) doped, and **d** 0.012 mol dm^{-3} Zn(II) doped

Kurtz powder SHG measurements

The second harmonic generation test on the crystals was performed by the Kurtz powder SHG method [46]. An Nd:YAG laser with modulated radiation of 1064 nm was used as the optical source and directed on the powdered sample through a filter. The grown crystals were ground to a uniform particle size of 125–150 μm and then packed in a micro capillary of uniform bore and exposed to laser radiation. The output from the sample was monochromated to collect the intensity of the 532 nm component and to eliminate the fundamental. Second harmonic radiation generated by the randomly oriented micro crystals was focused by a lens and detected by a photo multiplier tube.

Results and discussion

FT-IR spectral analysis

The FT-IR spectra were recorded for both the doped and undoped specimens using an AVATAR 330 FT-IR by KBr pellet technique in the range of 500–4000 cm^{-1} (Fig. 2). A very slight shift in some of the characteristic vibrational frequencies of pure KHP is observed because of doping with Zn(II).

XRD analysis

The powder X-ray diffraction (XRD) analysis was performed with a graphite monochromated Cu Kα radiation. XRD pattern of KHP crystals grown rapidly in Zn(II) added solution is compared with that of pure KHP crystal (Fig. 3). XRD profile of product is consistent with that of pure KHP crystal. No change in basic structure is observed. The XRD data is analyzed with Rietveld method with RIETAN-2000. The lattice parameters are, $a = 9.642$ Å, $b = 12.130$ Å, $c = 6.655$ Å, $\alpha = \beta = \gamma = 90°$. The lattice parameters are in agreement with reported values [47]. However, the relative intensities of the patterns differ. The corresponding peak intensity ratio (I/I_0) of pure KHP is markedly different from (I'/I_0) of the doped specimens. The change in intensity pattern reveals the lattice distortion by doping. The granularity of the crystals increases from 37 to 90 nm by low doping.

SEM and EDS analysis

SEM study gives information about the surface nature and its suitability for device fabrication. Also it is used to check the presence of imperfections. It has been reported that effectiveness of different impurities in changing the surface morphology is different. At low concentrations of dopants the effects are reflected by changes in configuration of grown structures. The SEM photograph of KHP (Fig. 4) shows deep crack developments on the surface. Incorporation of Zn(II) dopant into the crystalline matrix is observed by EDS and its concentration increases with increase in [Zn(II)] in the aqueous growth medium (Fig. 5). Analysis of surface at different sites reveals that the incorporation is nonuniform over the surface. Because of the smaller size of the dopant Zn(II) ($r = 88$ pm) compared with that of K^{1+} ($r = 152$ pm), it is expected to occupy the substitutional positions. Further, the substitution of bivalent zinc for the monovalent potassium will result in cation vacancies and crystal defects.

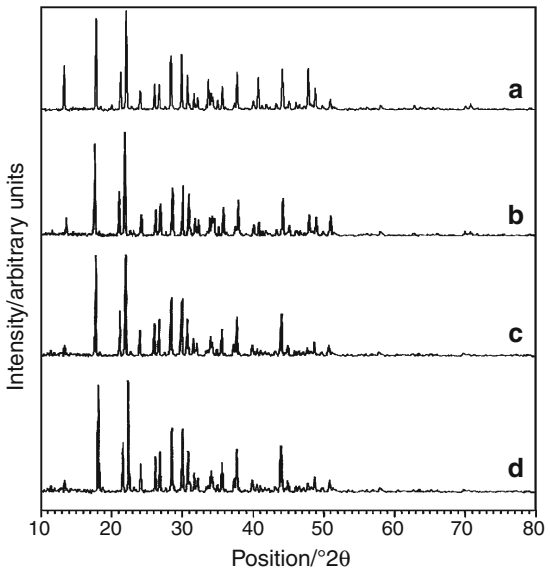

Fig. 3 Powder X-ray diffraction curves of KHP crystals. *a* Pure, *b* 0.0005 mol dm^{-3} Zn(II) doped, *c* 0.003 mol dm^{-3} Zn(II) doped, and *d* 0.012 mol dm^{-3} Zn(II) doped

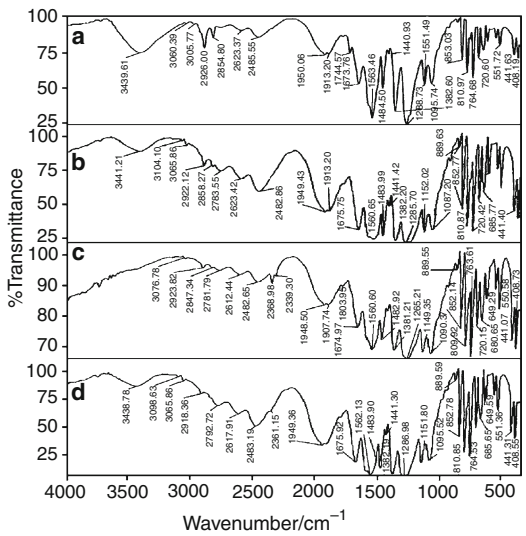

Fig. 2 FT-IR spectra of KHP crystals. *a* Pure, *b* 0.0005 mol dm^{-3} Zn(II) doped, *c* 0.003 mol dm^{-3} Zn(II) doped, and *d* 0.012 mol dm^{-3} Zn(II) doped

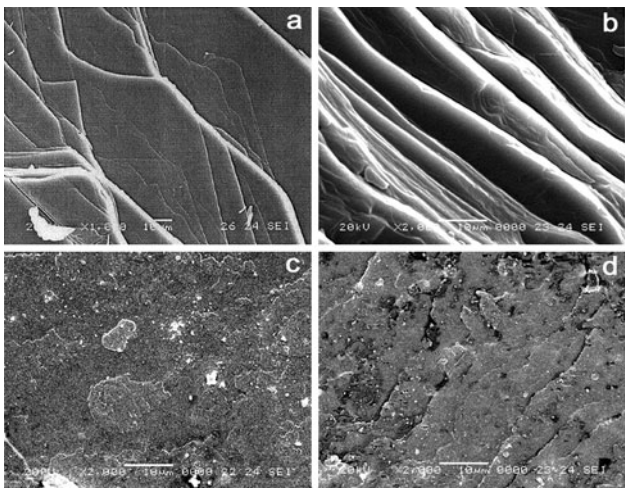

Fig. 4 SEM of KHP crystals. **a** Pure, **b** 0.0005 mol dm^{-3} Zn(II) doped, **c** 0.003 mol dm^{-3} Zn(II) doped, and **d** 0.012 mol dm^{-3} Zn(II) doped

Thermal analysis

The DSC and TG-DTA curves of pure KHP and heavily Zn(II)-doped KHP crystals are given in Figs. 6 and 7, respectively. The thermal analysis shows that there is no physically adsorbed water in the molecular structure of crystals grown from doped solution. Studies reveal the purity of the materials. Both DSC and DTA curves show sharp endothermic peaks at about 300 °C. TG curves show decomposition at around 300 °C with mass loss of almost 40% suggesting the sublimation of the compounds. No decomposition below the melting point (Figs. 6, 7) ensures the stability of the material for application in lasers where the crystals are required to withstand high temperatures. The changes in DSC and TG-DTA curves of heavily Zn(II)-doped KHP crystals suggest the incorporation of the dopant into the crystalline matrix.

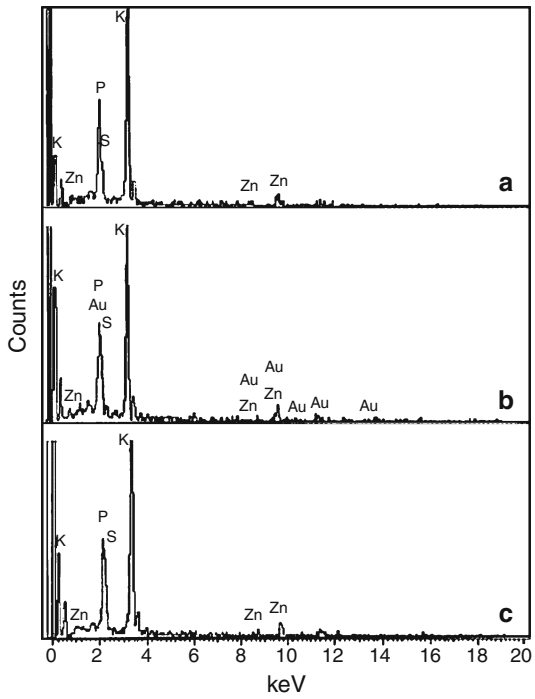

Fig. 5 EDS of KHP crystals. *a* 0.0005 mol dm^{-3} Zn(II) doped, *b* 0.003 mol dm^{-3} Zn(II) doped, and *c* 0.012 mol dm^{-3} Zn(II) doped

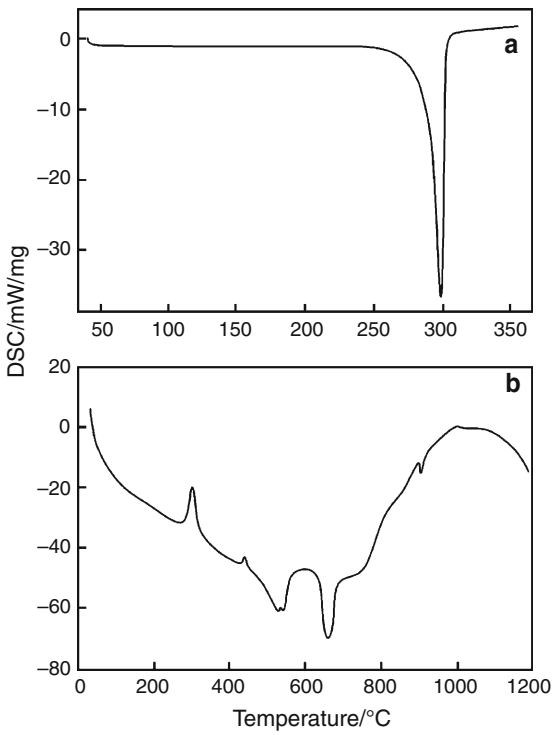

Fig. 6 DSC curves of **a** pure KHP and **b** heavily Zn(II)-doped KHP crystals (exo up)

UV–Vis and PL spectral studies

UV–Visible absorption spectra were recorded on a Hitachi UV–visible spectrometer in the spectral range 200–1000 nm for the pure and doped samples (Fig. 8). The optical transmissions are not altered much in the case of Zn(II) doping. The lower cut off wavelength remains almost same. High percentage of transmittance in the entire visible region is observed for all the samples.

Figure 9 represent the fluorescence spectra of KHP and heavily Zn(II)-doped KHP. It is observed that doping increases the fluorescence intensities. Shift in emission maximum is not appreciable.

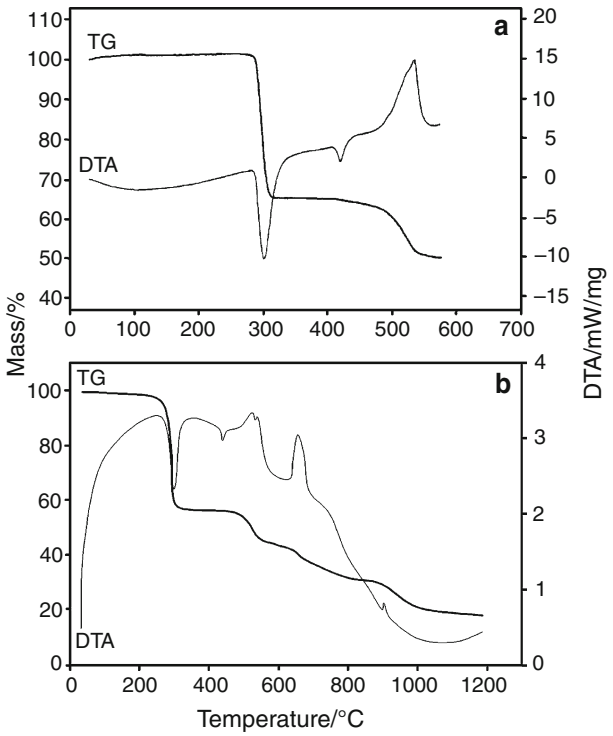

Fig. 7 TG-DTA curves of **a** pure KHP and **b** heavily Zn(II)-doped KHP crystals (exo up)

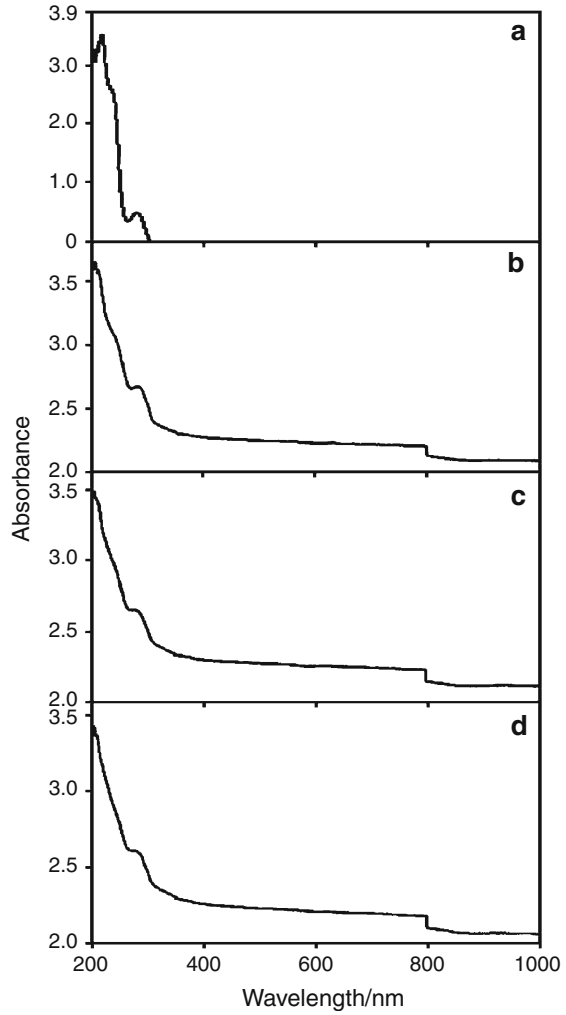

Fig. 8 UV–Vis spectra of KHP crystals. *a* Pure, *b* 0.0005 mol dm^{-3} Zn(II) doped, *c* 0.003 mol dm^{-3} Zn(II) doped, and *d* 0.012 mol dm^{-3} Zn(II) doped

SHG efficiency

Second harmonic generation test on crystal was performed by Kurtz powder SHG method [46]. An Nd:YAG laser with a modulated radiation of wavelength 1064 nm was used as the optional source and directed on powdered sample through a filter. The doubling of frequency was confirmed by green radiation of wavelength 532 nm. Although many materials have been identified that have higher molecular nonlinearities, the attainment of second order effects requires favorable alignment of molecule within the crystal structure. The efficient SHG demands specific molecular alignment of crystals to be achieved facilitating nonlinearity in the presence of dopant. It has been reported that SHG can be greatly enhanced by altering molecular alignment through inclusion complexation [48]. Intensity of second harmonic generation gives an indication of the NLO efficiency of the material. Zn(II) doping significantly improves the nonlinear optical property and hence it is a useful dopant (Table 1).

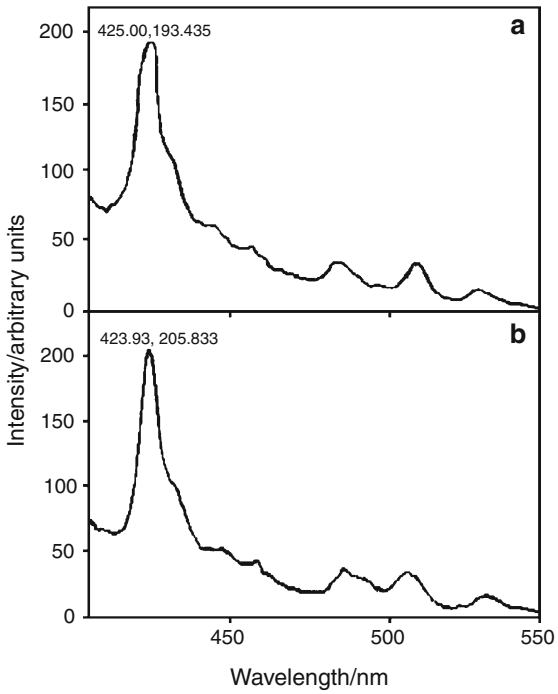

Fig. 9 Fluorescence spectra of *a* pure KHP and *b* Zn(II)-doped KHP

Table 1 SHG output

System	$I_{2\omega}$/mV
Pure KHP	27–29
Zn(II)-doped KHP	89–90

Conclusions

The influence of doping the transition metal, Zn(II) on KHP crystals has been studied. A close observation of FT-IR and XRD profiles of doped and undoped samples reveals some minor structural variations. These studies indicate that the crystal undergoes considerable lattice stress as a result of doping. Energy dispersive spectrum reveals the incorporation of Zn(II) in the crystalline matrix of KHP crystals. Small quantity additions of Zn(II) enhance the fluorescence intensity of KHP crystals. Doping results in morphological changes and significantly improves the SHG efficiency of the host crystal.

References

1. Jones JL, Paschen KW, Nicholson JB. J Appl Opt. 1963;2:955.
2. Yoda O, Miyashita A, Murakami K, Aoki S, Yamaguchi N. Proc SPIE Int Soc Opt Eng. 1991;1503:463.

3. Miniewicz A, Bartkiewicz S. Adv Mater Opt Electr. 1993;2:157.
4. Kejalakshmy N, Srinivasan K. Opt Mater. 2004;27:389.
5. Shankar MV, Varma KBR. Ferroelectr Lett Sect. 1996;21:55.
6. Okaya Y. Acta Crytallogr. 1965;19:8792.
7. Hottenhuis MHJ, Gardeniers JGE, Jetien LAMJ, Bennema P. J Cryst Growth. 1988;92:171.
8. Nisoli M, Pruneri V, Magni V, De Silvestri S, Dellepiane G, Cuniberti DC, et al. Appl Phys Lett. 1994;65:590.
9. Timpanaro S, Sassella A, Borghesi A, Porzio W, Fountaine P, Goldmann M. Adv Mater. 2001;13:127.
10. Van Enckevort WJP, Jetten LAMJ. J Cryst Growth. 1982;60:275.
11. Ester GR, Price R, Halfpenny PJ. J Cryst Growth. 1997;182:95.
12. Boubaker K. A comparative study of thermal properties of similar Zn free and Zn doped thin films. Curr Appl Phys. 2009. doi: 10.1016/j.cap.2009.02.016.
13. Streicher F, Sadewasser S, Enzenhofer T, Schock H-W, Lux-Steiner MCh. Thin Solid Films. 2009;517:2349.
14. Cheng XF, Leng WH, Liu DP, Zhang JQ, Cao CN. Chemosphere. 2007;68:1976.
15. Cheng G, Wu K, Zhao P, Cheng Y, He X, Huang K. J Cryst Growth. 2007;309:53.
16. Hussain M, Takita K. Phys C. 2007;467:120.
17. Bhagavannarayana G, Parthiban S, Chandrasekaran C, Meenakshisundaram SP. Cryst Eng Commun (in press).
18. Bhagavannarayana G, Parthiban S, Meenakshisundaram S. Cryst Growth Design. 2007;8:446.
19. Bhagavannarayana G, Kushwaha S, Parthiban S, Meenakshisundaram S. J Cryst Growth. 2009;311:960.
20. Meenakshisundram S, Parthiban S, Bhagavannarayana G, Madhurambal G, Mojumdar SC. J Therm Anal Calorim. 2009;96:125.
21. Swiderski G, Kalinowska M, Wojtulewski S, Lewandowski W. Spectrochim Acta A. 2006;64:24.
22. Flakus HT, Jablonska M. J Mol Struct. 2004;707:97.
23. Hanai K, Kuwae A, Takai T, Senda H, Kunimoto K. Spectrochim Acta A. 2001;57:513.
24. Hsich T-J, Su C-C, Su C-C, Chen C-Y, Liou C-H, Lu L-H. J Mol Struct. 2005;741:193.
25. Vasudevan G, Anbusrinivasan P, Madhurambal G, Mojumdar SC. J Therm Anal Calorim. 2009;96:99.
26. Julg A, Francois P. Theor Chim Acta. 1967;7:24.
27. Kalinowska M, Siemieniuk E, Kostro A, Lewandowski W. J Mol Struct. 2006;761:129.
28. Anbusrinivasan P, Madhurambal G, Mojumdar SC. J Therm Anal Calorim. 2009;96:111.
29. Varsanyi G. Assignments for Vibrational Spectra of 700 Benzene Derivatives. Budapest: Academiai Kiado; 1973.
30. Reva ID, Stepanian SG. J Mol Struct. 1995;349:337.
31. Spanian SG, Reva ID, Radchenko ED, Sheina GG. Vib Spectrosc. 1996;11:123.
32. Wienda DA, Feng TL, Barron AR. Acta Crystallogr C. 1989;45:338.
33. Bryan RF, Fryeberg DP. J Chem Soc Perkin Trans. 1975;2:1825.
34. Madhurambal G, Mojumdar SC, Hariharan S, Ramasamy P. J Therm Anal Calorim. 2004;78:125.
35. Lewandowski W, Dasiewicz B, Koczon P, Skierski J, Dobrosz-Teperek K, Swislocka R, et al. J Mol Struct. 2002;604:189.
36. Lewandowski W. Can J Spectrosc. 1987;32:41.
37. Dichi P, Kellerhals M, Lounila J, Wasser R, Hiltunen Y, Jokisari J, et al. Magn Res Chem. 2005;25:244.
38. Mojumdar SC. J Therm Anal Calorim. 2001;64:629.
39. Chenthamarai S. Cryst Eng. 2001;4:37.
40. Hameed SH, Ravi G, Dhanasekaran R, Ramasamy P. J Cryst Growth. 2000;212:227.
41. Patel RN, Pandeya KB. J Inorg Biochem. 1998;71:109.
42. Rathore HS, Varshney G, Mojumdar SC, Saleh MT. J Therm Anal Calorim. 2007;90:681.
43. Mojumdar SC, Sain M, Prasad R, Sun L, Venart JES. J Therm Anal Calorim. 2008;90:653.
44. Mojumdar SC, Lebruskova K, Valigura. Chem Pap. 2003;57:245.
45. Mojumdar SC, Capek I, Capek P, Fialova L, Berek D. Res J Chem Environ. 2007;11:5.
46. Kurtz SK, Perry TT. J Appl Phys. 1968;39:3798.
47. Murugakoothan P, Mohankumar R, Ushashree PM, Jayavel R, Dhansekaran R, Ramasamy P. J Cryst Growth. 1999;207:325.
48. Wang Y, Eaton DF. Chem Phys Lett. 1985;120:441.